Magnetization reversal and anomalous coercive field temperature dependence in MnAs epilayers grown on GaAs(100) and GaAs(111)B

L. B. Steren,[1] J. Milano,[1] V. Garcia,[2] M. Marangolo,[2] M. Eddrief,[2] and V. H. Etgens[2]

[1] *Centro Atómico Bariloche, CNEA-UNC, (8400) S.C. de Bariloche, Argentina.*
[2] *Institut des NanoSciences de Paris, INSP, Université Pierre et Marie Curie-Paris 6, Université Denis Diderot-Paris 7, CNRS UMR 7588, Campus Boucicaut, 140 rue de Lourmel, 75015 Paris, France.*

(Dated: February 6, 2008)

The magnetic properties of MnAs epilayers have been investigated for two different substrate orientations: GaAs(100) and GaAs(111). We have analyzed the magnetization reversal under magnetic field at low temperatures, determining the anisotropy of the films. The results, based on the shape of the magnetization loops, suggest a domain movement mechanism for both types of samples. The temperature dependence of the coercivity of the films has been also examined, displaying a generic anomalous reentrant behavior at T>200 K. This feature is independent of the substrate orientation and films thickness and may be associated to the appearance of new pinning centers due to the nucleation of the β-phase at high temperatures.

PACS numbers: 73.70.Ak ; 75.60.-d ; 75.30.Gw ; 75.30.Kz

I. INTRODUCTION

In the last few years, a lot of effort has been invested to understand the physical properties of MnAs-based thin films and multilayers. Bulk manganese arsenide is ferromagnetic at room temperature with a NiAs hexagonal structure (α-phase).[1,2,3] At T_C =313 K however, MnAs displays a first-order phase transition that drives the system to a paramagnetic state. At this temperature, a structural transition occurs from the low-temperature α-phase to an orthorhombically-distorted (MnP) β-phase. At T_{St} =398 K, a second structural transition takes place and the system regains a NiAs hexagonal structure. MnAs grows epitaxially on various standard semiconductor substrates such as GaAs(100),[4,5,6] GaAs(111)B,[7,8,9] GaAs(110),[10] InP(100),[11] Si(100)[12] and Si(111).[13] The excellent quality of MnAs/GaAs heterostructures makes this compound particularly interesting for hybrid metal/semiconductor spintronics.[14,15,16,17]

The epitaxy introduces strain and defects in MnAs thin films that significatively modify their structural and magnetic properties with repect to the bulk. When MnAs is grown on GaAs(100) or GaAs(111)B, epitaxial strain induces an α/β-phases coexistence in a wide range of temperature.[9,18] In addition, the T_C of the thin films can be enhanced when they are grown on GaAs(111)B substrates.[9] The orientation of the GaAs substrate determines the growth behavior and epilayer orientation. When grown on GaAs(111)B substrate, MnAs lies with the hexagonal c axis aligned with the growth direction [Fig. 1(b)];[7] while for the growth on GaAs(100) substrate, two orientations of the epilayer have been described.[4] By correctly adjusting the growth conditions, it becomes possible to obtain one single phase[19] with the MnAs *c*-axis parallel to the GaAs [110] that lies inside the surface plane [Fig. 1(b)]. Due to the important misfit between the thin film and the substrate (7%), the epilayer relaxes its strain from the very beginning of the growth. Above a certain thickness, the epilayer is expected to be fully relaxed at the growth temperature. However, during the after-growth cooling cycle, a residual strain is introduced due to the large dilatation coefficients difference between MnAs and GaAs.[20] In fact, as the $\alpha - \beta$ phase transition proceeds mainly by a 1% lattice parameter contraction in the hexagonal plane, strain will accommodate differently for MnAs/GaAs(100) or MnAs/GaAs(111)B.

Another particularity of MnAs epilayers grown on GaAs(100) substrates is that, within the phase coexistence region, scanning tunneling microscopy (STM) images show the presence of stripes along the [0001] direction with two different heights, arranged alternated within the $[11\bar{2}0]$ direction.[21] Magnetic force magnetometry (MFM) studies indicate that the higher stripes are ferromagnetic (α-phase) while the shallower are paramagnetic (β-phase).[22] X-ray diffraction (XRD) patterns also agree with the α-β phase coexistence in the 280-314 K temperature range. No stripes are however observed for MnAs epilayers grown on GaAs(111)B. Instead, the surface morphology shows triangular and sticks features depending on the growth parameters like substrate temperature, As overpressure, etc.[23] Even if no stripes are visible, the phase coexistence has been unambiguously observed between 296 and 328 K by XRD for this orientation.[9]

In the present work, we perform a detailed study of the magnetism of MnAs epilayers, grown on both GaAs(100) and GaAs(111)B substrate orientations. The anisotropy of the films is analyzed in terms of magneto-crystalline and substrate-induced anisotropy terms. The temperature dependence of the coercivity of the films is measured and explained in terms of thermally activated domain-wall movements and the appearance of new pinning centers.

II. EXPERIMENTAL DETAILS AND CHARACTERIZATION OF THE SAMPLES

MnAs epilayers are grown by molecular beam epitaxy (MBE) with a substrate temperature of about 240°C on previously prepared GaAs buffer layers. After removal of the native oxide, a very thin buffer layer is grown on GaAs(111)B substrates[24] while a standard 100 nm thick buffer layer is grown on GaAs(100). Each MnAs growth begins under As rich conditions on the GaAs buffer layer. Different epilayer thicknesses, t_x, ranging from 30 nm to 200 nm, are grown on both (100) and (111) substrate orientations. The films are named M100-t [nm] and M111-t [nm], respectively. Finally, the samples are capped *in situ* with an amorphous ZnSe layer.

Magnetization vs. temperature and magnetic field curves are measured in a vibrating sample magnetometer (VSM) and a superconducting quantum interference device magnetometer (SQUID). The temperature is varied from 5 K to 300 K and the magnetic fields swept up to 5 T. The magnetization loops are measured with the magnetic field rotating in the plane of the film (IP) $\theta_H = \pi/2$ and in the out-of-plane geometry (OOP), keeping the azimuthal angle φ_H fixed [Fig. 1(a)].

III. RESULTS AND DISCUSSION

The ferromagnetic phase with hexagonal structure displays a strong anisotropy with a hard-axis parallel to the c-axis, that favors the orientation of the magnetization in a plane perpendicular to this direction.[25] As mentioned previously, the hexagonal c-axis is inside the plane of the films for M100 samples and perpendicular to it for M111 samples [Fig. 1(b)], which strongly affects the magnetism of the samples. The magnetization loops reflect the structural stacking of MnAs in the films. Fig. 2 shows the typical magnetization loops for M100 and M111 samples. These have been measured in three different configurations of the applied field: in-the-plane of the films and parallel to the x-axis, IP-PA ($\theta_H = \pi/2$, $\varphi_H = 0$), in-plane and perpendicular to the x-axis, IP-PE ($\theta_H = \pi/2$, $\varphi_H = \pi/2$) and out-of-the-plane of the films with $\theta_H = 0$. The x-axis is parallel to the $[11\bar{2}0]$ axis for M100 samples, and is not clearly determined for M111 samples.

Fig. 2(a) evidences the existence of a strong uniaxial anisotropy in the plane of M100 films, with the easy-axis oriented along the MnAs $[11\bar{2}0]$ direction. The saturation field of the in-plane curve, measured with the magnetic field perpendicular to the easy-axis direction, is much larger than the OOP one, indicating that the anisotropy term overcomes the demagnetization effect in these films. In M111 films [Fig. 2(b)] and due to the structure stacking onto the substrate, the hard axis strengthens the demagnetization effect favoring an almost isotropic in-plane magnetization.

The free energy density proposed is:

$$F_{100} = -\vec{M}.\vec{H} + K_1 \sin^2\theta . \sin^2\varphi + K_n \cos^2\theta + 2\pi M_S \cos^2\theta \quad (1)$$

$$F_{111} = -\vec{M}.\vec{H} + K_1 \cos^2\theta + 2\pi M_S \cos^2\theta + \mathcal{O}^2(K_2(\varphi)) \quad (2)$$

for M100 and M111 samples, respectively.

The first term in each equation accounts for the Zeeman energy and the second term includes a uniaxial anisotropy oriented in the plane of the film or out of the plane, depending on the samples substrate orientation. The last term represents the magnetostatic energy. To describe the experimental results we have included an extra anisotropy term in the M100 energy expression, K_n, that favors an in-plane magnetization. We associate this contribution to substrate-induced strains onto the film structure. In Ref. 18 A.K. Das and coworkers already reported that the ferromagnetic phase is orthorhombically distorted at the coexistence region of α-MnAs and β-MnAs. The existence of such anisotropy in M111 films could not be deduced from our measurements. This contribution may be hidden by the demagnetizing and the uniaxial anisotropy terms. The study of thinner films is needed to define the role of this contribution in the magnetization of MnAs films. Corrections of higher order to the in-plane anisotropy of M111 samples are needed to describe the experimental results. These terms are highly samples dependent, as discussed below.

The uniaxial anisotropy constant, K_1 was calculated from the area enclosed by the loops measured along the easy and the hard directions. The demagnetization term is calculated taking Ms=870 emu/cm^3, as deduced from the magnetization vs. temperature measurements. The calculated anisotropy constants are $K_1 = 1.3 \times 10^6$ J/m^3 and $K_n = 1.5 \times 10^5$ J/m^3 for M100 samples and $K_1 = 1.3 \times 10^6$ J/m^3 for M111 ones. The uniaxial anisotropy, K_1, is of magneto-crystalline origin and agrees well with the values measured by J. Lindner *et al.*[26] K_1 does not depend notably on the thickness of the samples or the substrate orientation and is very close to the bulk value.[25]

In Fig. 3, the hysteretic zone of the loops measured with the magnetic field applied along the in-plane easy-axis is shown. The shape of the loops of M111 and M100 samples are notably different. While in M111 samples [Fig. 3(b)] the magnetization reversal is smooth, the magnetization in M100 ones [Fig. 3(a)] shows a sharp jump at the coercive field where a partial inversion of the magnetization occurs, while higher magnetic fields are necessary to completely saturate the magnetization of the sample. The shapes of the curves are associated with domains movements and are affected both by defects and other inhomogeneities and by the anisotropy of the samples.[27] The coercivity increases as the thickness of the films decreases, indicating that the magnetization reversal is affected by substrate-induced strains and topographic defects.

In M100 samples, the coercivity of the loops measured

along the easy-axis, $H_c(0)$ follows the condition:

$$H_c(0) \ll K/M, \tag{3}$$

indicating that the magnetization reversal is mainly driven by domain wall movement.

In M111 samples, the in-plane anisotropy terms are much smaller and condition (3) is no longer valid. The direction perpendicular to the film surface is a very strong hard-axis due to the superposition of the magneto-crystalline anisotropy and the demagnetizing field resulting in large domain walls. For this reason we suggest that the walls in this system are Néel-like, i.e., the magnetization within the walls rotates in the film plane. A simple calculation of domain wall widths, δ, in M111 films based on the effective anisotropy of the system results in $\delta > t$ values. According to the Néel criteria, in this case the wall mode using an in-plane rotation has a lower energy than the classical Bloch mode.[28]

The in-plane angular dependence of the magnetization loops has been carefully measured by VSM. We observe that the magnetization loops of M100 samples change remarkably as the magnetic field is rotated in the plane of the films while those of M111 samples vary very little. The magnetic remanence vs. the azimuthal angle, φ curves underlines the symmetry of the magnetic anisotropy of the films. M100 samples show a strong uniaxial anisotropy with a hard-axis oriented along [0001] direction. M111 samples, on the other hand, present a much weaker anisotropy contribution with different symmetries, depending on the growth conditions. Uniaxial, three and four-fold anisotropy symmetries have been observed in different samples. Typical $H_c(\varphi)$ curves for M100 and M111 samples are shown in Fig. 4.

The coercivity of M100 films shows two high peaks at both sides of the hard-axis angle. The angular dependence of H_c for $0 < \varphi < \pi/2$ can be fitted by:[29]

$$cos\varphi = H_c(0)/H_c(\varphi) \tag{4}$$

suggesting that the magnetization reversal is driven by 180^o wall movements [inset Fig. 4(a)]. In a recent article, F. Schippan and coworkers[30] report MFM images that show in similar samples the existence of 180^o walls, oriented along the $[11\bar{2}0]$ direction. As the uniaxial in-plane anisotropy is much larger than the demagnetizing term, the walls are Bloch-like, i.e. the magnetization in the walls rotates out-of-the-plane of the films. Even if MFM measurements have been performed at room temperature where the α and the β phases coexist, these results are a strong indication of the domain configuration in these samples.

The φ dependence of the H_c is much weaker for M111 samples and has a four-fold anisotropy in the case of the M111-66 film shown in Fig. 4(b). The symmetry of the in-plane anisotropy in these samples can be three-fold and even two-fold and is strongly dependent on the sample growth parameters: substrate temperature during sample growth, surface stoichiometry, etc. The origin of this term may be associated to surface-induced strains and/or surface reconstruction symmetries. A study of the anisotropy of M111 ultrathin films is under progress to clarify this point.

The OOP angular dependence of M100 and M111 coercive fields is shown in Fig. 5. An important increase of the coercive field with angle is observed, as the field approaches the film normal direction. The coercivity abruptly decreases to zero at the hard-axis of magnetization. M100 and M111 samples display a similar behavior, following a $H_c(0)/cos(\theta)$ function. The remanence monotonically decreases to zero as θ is varied from $\pi/2$ to 0, keeping φ fixed and parallel to the in-plane easy axis direction. As condition (3) is fulfilled in this geometry for both group of samples, the reversal process can be thought as performed with only the component of the external field parallel to the easy-axis magnetization direction.

The temperature dependence of the coercive field, extracted from loops measured with the applied field oriented along the in-plane easy-axis was examined (Fig. 6). At low temperatures, T$\leq$200 K, the coercive field decreases smoothly with increasing temperature, as expected for an ordinary ferromagnet. This behavior is understood in terms of thermal activation of domain walls.[31] At T_I $\sim$200 K, this tendency is reversed and an increase of the H_c is observed, up to T_{II} $\sim$300 K. This anomalous behavior is associated to the appearance of new pinning centers. These new pinning sites would progressively appear as the temperature increases at nucleation points of the β-phase or strained regions of the α-phase. Previous papers report the α-β phase coexistence in both type of samples but at higher temperatures.[9,22]

The magnetization vs. temperature curves do not show any particular feature in the T_I - T_{II} range (see Inset of Fig. 6). Ferromagnetic resonance measurements indicate that the magneto-crystalline anisotropy decreases with temperature as the system approaches the Curie temperature, T_C,[32] without showing noticeable signatures around 200 K. Therefore, the magneto-crystalline anisotropy of MnAs cannot be the origin of the observed effect. The M vs. T curve saturates at low temperatures to the bulk moment[3] but an important increase of the Curie temperature, T_C, from 314 K to 330 K (M100) and 350 K (M111), is observed. This result suggests that the strains induced by the GaAs stabilize the α-hexagonal phase up to this high temperature. In fact, X-ray[9] and neutron[33] diffraction patterns show a α-β coexistence in the 314 K- T_C temperature range for M111 samples. Thus, in this temperature range, the magnetization would be given by the addition of an unsaturated ferromagnetic component that corresponds to the α-phase and a paramagnetic contribution, arising from the β phase. Finally, above room temperature the thermal energy overcomes the effect of the new pinning centers and induces a strong reduction of the coercive field as the temperature approaches T_C.

Data shown in Fig. 6 evidence that the reentrant ef-

fect is independent of the substrate orientation. The observed behavior in the coercivity could then be associated to a former stage of the α-β phase coexistence. A. Ney *et al.*[34] first observed this anomalous behavior in M100 films and associated it to the existence of an array of α-MnAs stripes. The authors claim that the temperature dependence of the coercivity allows them to distinguish between homogeneous and stripes domains of α-MnAs. However, STM images show that M111 samples do not form ferromagnetic stripes at room temperature.[23] Our finding of a similar behavior in both types of samples suggests that the origin of this effect does not reside in the appearance of the α-phase in the form of stripes but in the phase coexistence phenomena, beyond the epitaxy between MnAs and GaAs. The number of pinning centers is temperature dependent due to the progressive nucleation of β-phase regions and/or the strain evolution in the α phase towards the phase transformation.

Fig. 7 shows the temperature dependence of the coercivity for M100 samples of different thicknesses. The increase of the H_c with temperature, in the T_I - T_{II} zone is more pronounced for thinner films. However, the functional form of the temperature variation of the coercivity does not depend on thickness.

The results indicate, in summary, that even though the coercivity in this case is essentially given by extrinsic properties, the reentrant behavior seems to be an intrinsic characteristic of the magnetism of MnAs thin films.

IV. CONCLUSIONS

We have shown that the magnetization reversal in MnAs films depends on the substrate orientation and is strongly affected by the magneto-crystalline anisotropy of the compound.

On one hand, the angular dependence of the coercive field of films grown on GaAs(100) shows that the in-plane magnetization reversal occurs by 180^0 domain wall movements. Moreover, the shape of the hysteresis loops indicates that the magnetization alignment with the magnetic field is driven in two-steps. This is explained by the existence of a distribution of potential barriers for domain movement, that have a very sharp threshold at the coercive field where more than 70% of the magnetization turns into the direction of the applied field. The magnetization alignment is strongly affected by the in-plane hard uniaxial anisotropy of the system, that induces the formation of Bloch walls along the films.

On the other hand the uniaxial anisotropy of samples grown on GaAs(111)B is oriented perpendicular to the film surface, leading to the creation of Néel domain walls and a smooth reversal of the magnetization in a low-field range.

Summarizing, we have demonstrated that the coercivity of the films presents a general anomalous behavior as a function of temperature, independent of the substrate orientation and films thicknesses. This effect is associated to the appearance of new pinning centers as a consequence of the progressive growth of a β-phase or distortion of the α-phase as the temperature is increased above 200 K.

V. ACKNOWLEDGEMENTS

The authors thank partial financial support from Fundación Antorchas, FONCyT 03-13297, Universidad Nacional de Cuyo, CONICET and the ECOS-SUD.

[1] R.H. Wilson and J.S. Kasper, Acta Crystallogr. **17**, 95 (1964).
[2] B.T.M. Willis and H, Rooksby, Proc. Phys. Soc. B **67**, 290 (1954).
[3] J.B. Goodenough and J.A. Kafalas, Phys. Rev. **157**, 389 (1967).
[4] M. Tanaka, J.P. Harbison, M.C. Park, Y.S. Park, T. Shin and G. M. Rothberg, Appl. Phys. Lett. **65**, 1964 (1994).
[5] A. Trampert, F. Schippan, L. Däweritz and K.H. Ploog, Appl. Phys. Lett. **78**, 2461 (2001).
[6] S.H. Chun, S.J. Potashnik, K.C. Ku, J.J. Berry, P. Schiffer and N. Samarth, Appl. Phys. Lett. **78**, 2530 (2001).
[7] M. Tanaka, K. Saito and T. Nishinaga, Appl. Phys. Lett. **74**, 64 (1999).
[8] B. Jenichen, V.M. Kaganera, M. A. Kästner, C. Herrmann, L. Däweritz, R. Noch, K.H. Ploog, Phys. Rev. Lett. **91**, 87203 (2003).
[9] N. Mattoso, M. Eddrief, J. Varalda, A. Ouerghi, D. Demaille and V.H. Etgens; Phys. Rev.B **70**, 115324 (2004).
[10] D. Kolovos-Vellianitis, C. Herrmann, L. Däweritz and K.H. Ploog, Appl. Phys. Lett. **87**, 092505 (2005).
[11] M. Yokoyama, S. Ohya, M. Tanaka, Appl. Phys. Lett. **88**, 012504 (2006).
[12] K. Akeura, M. Tanaka, M. Ueki and T. Nishinaga, Appl. Phys. Lett. **67**, 3349 (1995).
[13] A.M. Nazmul, A.G. Banshchikov, H. Shimizu, M. Tanaka, J. Cryst. Growth **227-228**, 874881 (2001).
[14] M. Tanaka, Semicond. Sci. Technol. **17**, 327 (2002).
[15] M. Ramsteiner, H. Y. Hao, A. Kawaharazuka, H. J. Zhu, M. A. Kästner, R. Hey, L. Däweritz, H.T. Grahn, K.H. Ploog, Phys. Rev. B **66**, 081304(R) (2002).
[16] S.H. Chun, S.J. Potashnik, K.C. Ku, P. Schiffer, N. Samarth, Phys. Rev. B **66**, 100408 (2002).
[17] V. Garcia, H. Jaffres, M. Eddrief, M. Marangolo, V.H. Etgens, J.M. George, Phys. Rev. B **72**, 081303(R) (2005).
[18] A.K. Das, C. Pampuch, A. Ney, T. Hesjedal, L. Däweritz,K.H. Ploog, N. Darowski and I. Zizak, Phys. Rev. B **68**, 132301 (2003).
[19] F. Schippan, A. Trampert, L. Däweritz and K. Ploog, J. Vac. Sci. Technol. B **17**, 1716 (1999).
[20] F. Iikawa, P.V. Santos, M. Kästner, F. Schippan, L. Däweritz, Phys. Rev. B **65**, 205328 (2002).

[21] T. Plake, M. Ramsteiner, M. Kästner, L. Däweritz, K.H. Ploog, Appl. Phys. Lett. **80**, 2523 (2002).
[22] L. Däweritz, L. Wan, B. Jenichen, C. Herrmann, J. Mohanty, A. Trampert, K.H. Ploog, J. Appl. Phys. **96**, 5056 (2004)
[23] A. Ouerghi, M. Marangolo, M. Eddrief, S. Guyard, V.H. Etgens; Phys. Rev.B **68**, 115309 (2003).
[24] V. Garcia, M. Marangolo, M. Eddrief, H. Jaffres, J.M. George, V.H. Etgens, Phys. Rev. B **73**, 035308 (2006).
[25] R.W. De Blois and D.S. Rodbell, Phys. Rev. **130**, 1347 (1963).
[26] J. Lindner, T. Tolinski, K. Lenz, E. Kosubek, H. Wende, K. Babershke, A. Ney, T. Hesjedal, C. Pampuch, R. Koch, L. Däweritz, K.H. Ploog, J.Magn.Magn.Mater.**277**, 159 (2004).
[27] E.A. Jagla, Phys. Rev.B **72**, 1 (2005).
[28] A. Hubert, R. Schäfer, *Magnetic Domains*, (Springer, Berlin 2000).
[29] S. Reich, S. Shtrikman, D. Treves; J. Appl. Phys. **36**, 140 (1965).
[30] F. Schippan, G. Behme, L. Däweritz, K. Ploog, B. Dennis, K. Neumann, K. Ziebeck, J. Appl. Phys. **88**, 2766 (2000).
[31] P. Gaunt and C.K. Mylvaganam, Phil. Mag. B **39**, 313 (1979).
[32] J. Milano, L.B. Steren, M. Marangolo, M. Eddrief, V.H. Etgens (unpublished).
[33] V. Garcia, Y. Sidis, M. Marangolo, M. Eddrief, F. Ott and V.H. Etgens (unpublished).
[34] A. Ney, T. Hesjedal, C. Pampuch, A.K. Das, L. Däweritz, R. Koch, K.H. Ploog, Phys. Rev.B **69**, 081306R (2004).

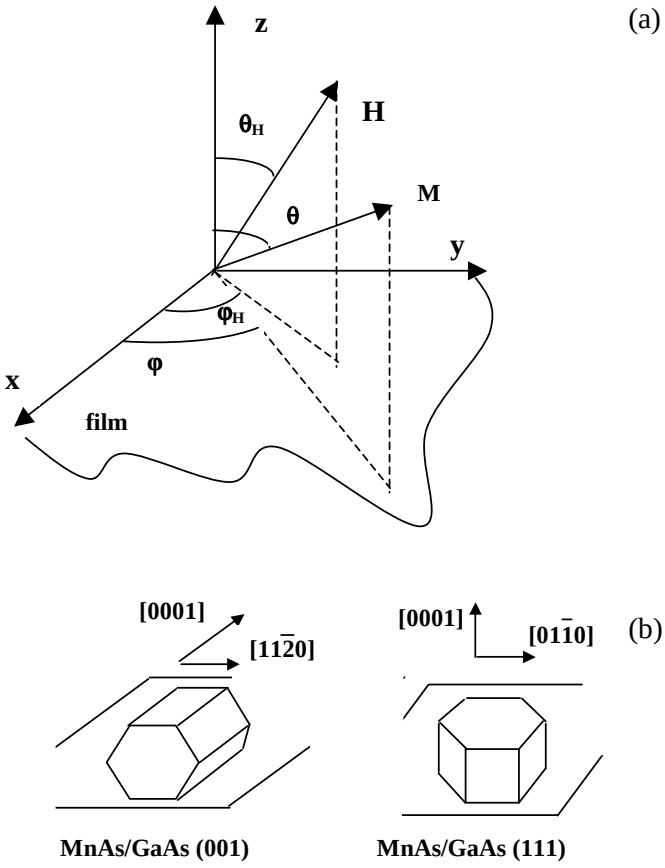

(a)

(b)

FIG. 1: (a) Coordinate system used in the paper; (b) Schematic view of the epitaxial relationship of MnAs on GaAs(100) and GaAs(111), respectively.

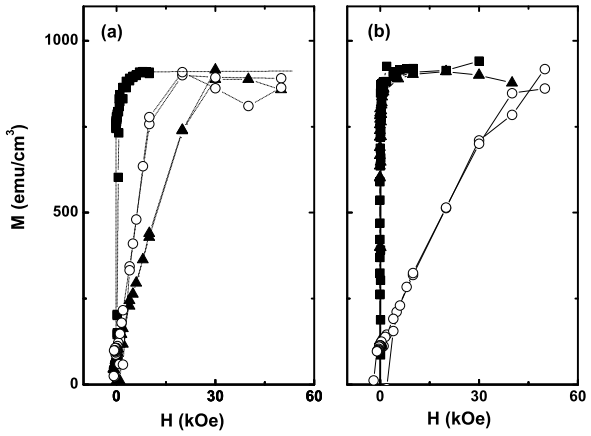

FIG. 2: Magnetization loops of (a) M100-66 and (b) M111-66 films measured with (▲) the magnetic field applied in the plane of the films and perpendicular to the x-axis, (■) in-plane and parallel to the x-axis and (◯) out-of- the plane of the films. The measurements were performed at 5 K in the SQUID magnetometer.

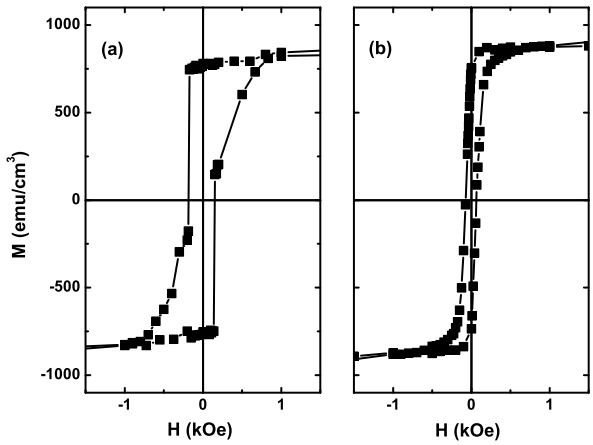

FIG. 3: Low-field detail of the hysteresis measured with the applied field oriented along the easy-axis for (a)M100-66, (b) M111-66. The measurements were performed at 5 K in the SQUID magnetometer.

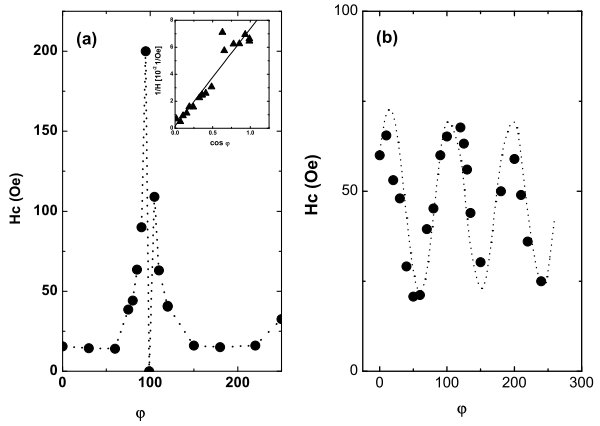

FIG. 4: Angular dependence of the coercivity, measured with the field rotating in the plane of the films. (a)M111-66, (b) M100-66. Measurements performed at 85 K in the VSM.

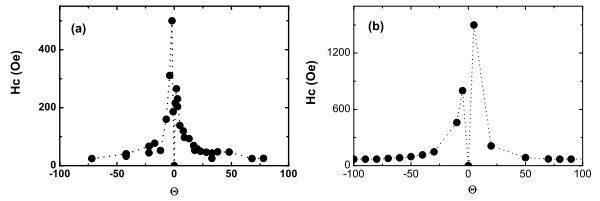

FIG. 5: Angular dependence of the coercivity measured in the OOP geometry. (a)M111-66, (b) M100-66. Measurements performed at 85 K in the VSM.

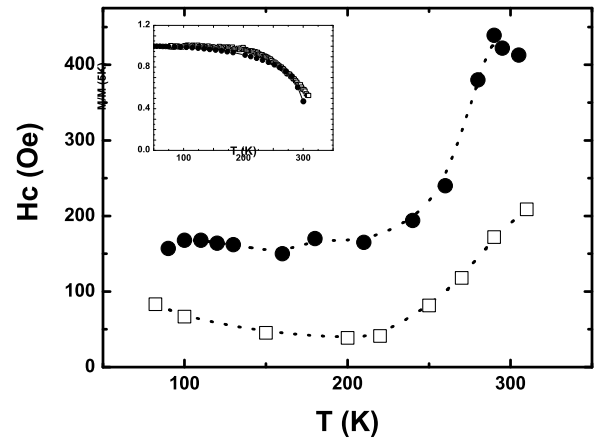

FIG. 6: Coercive field vs. temperature for (□) M111-66 and (•) M100-66 samples. Data taken from VSM measurements. Inset of the figure: M vs. T for (□) M111-100 and the (•) M100-100 samples, respectively.

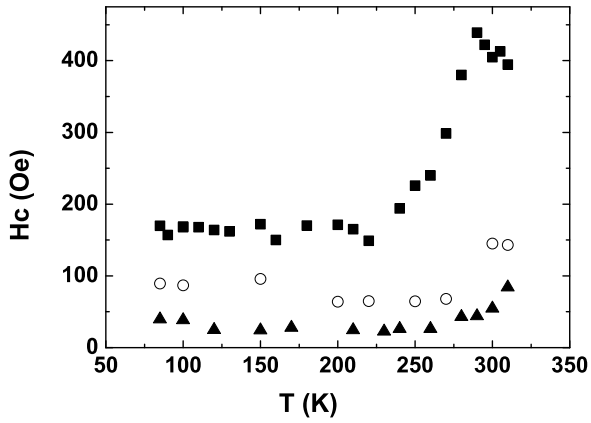

FIG. 7: Coercive field vs. temperature for (■) M100-66, (◯) M100-100 and (▲) M100-200 samples. Data taken from VSM measurements.